Journal of Electroceramics, 13, 585–591, 2004

Development of a New MnZn-Ferrite Soft Magnetic Material for High Temperature Power Applications

V. ZASPALIS,[1,*] V. TSAKALOUDI,[1] E. PAPAZOGLOU,[1] M. KOLENBRANDER,[2] R. GUENTHER,[2] & P. VAN DER VALK[3]

[1] *Center for Research and Technology-Hellas, Institute of Chemical Process Engineering, Laboratory of Inorganic Materials, P.O. Box 361, 57001 Thessaloniki, Greece*

[2] *Ferroxcube Deutschland GmbH, Department of Materials and Process Development, Essener Str. 4, 22419 Hamburg, Germany*

[3] *Ferroxcube International, Department of Advanced Product Design, Hurksetraat 19, 5652AH Eindhoven, the Netherlands*

Submitted February 10, 2003; Revised June 30, 2003; Accepted July 2, 2003

Abstract. At power electronic applications (e.g. in automotive, lighting, electrical equipment etc.) the inductive components that consist the heart of the power transformers are made of ceramic ferromagnetic materials of the type $(Mn_xZn_yFe^{2+}_{1-x-y})Fe^{3+}_2O_4$. Usually they are designed in such a way in order to exhibit optimum magnetic performance and electromagnetic power loss minimum at 80–100°C, which is the steady state operation temperature region for most devices. However, the continuous miniaturization of electric and electronic equipment associated with a continuous increase in the density of electronic components has as unavoidable consequence the gradual shift of the steady state operation temperature to higher levels. The need is therefore becoming obvious for the development of new power soft magnetic materials optimized to operate at higher temperatures than those at which current existing materials operate. In the present work the development is described of such a new soft ferrite material having the chemical composition $(Mn_{0.76}Zn_{0.17}Fe^{2+}_{0.07})Fe^{3+}_2O_4$, initial magnetic permeability of 1800 (measured at a frequency $f = 10$ kHz, an induction level $B < 0.1$ mT and a temperature $T = 25$°C), Curie temperature of 225°C and electromagnetic power losses <350 mW/cm^3 measured at a temperature of 140°C, frequency of 100 kHz and a magnetic field strength of 200 mT. The material has been successfully introduced to production and is now commercially available. The largest application is offered by the automotive industry in particular for tackling high temperature operating problems arising when control is being done near the engine (near the engine electronics).

Keywords: electromagnetic ceramics, soft-ferrites, MnZn-ferrites

Introduction

Ceramic ferromagnetic materials of the MnZn-ferrite family are the most broadly known category of soft electromagnetic materials. They are polycrystalline materials crystallized in the cubic structure similar to that of the mineral "spinel". Their magnetic properties arise from interactions between the magnetic dipoles of the metallic ions (i.e. Fe, Mn), that have uncompensated spin electrons and therefore net magnetic moments, occupying certain positions in relation to the oxygen ions in the crystal lattice [1]. MnZn-ferrites find various applications in devices that can be basically characterized as inductors, transformers and absorbers and can be found almost in all broad consumption electric, electronic or telecommunication equipment (e.g. Fig. 1).

Besides the magnetic permeability which is a necessary property for the existence of a magnetic component, another important parameter for the operation of MnZn-ferrite magnetic components, particularly in high power transformer applications, is the magnitude of the electromagnetic power losses. Those express the amount of electromagnetic energy not being transformed inductively into useful energy but dissipated inside the material in the form of heat. The total power

*To whom all correspondence should be addressed. E-mail: zaspalis@cperi.certh.gr

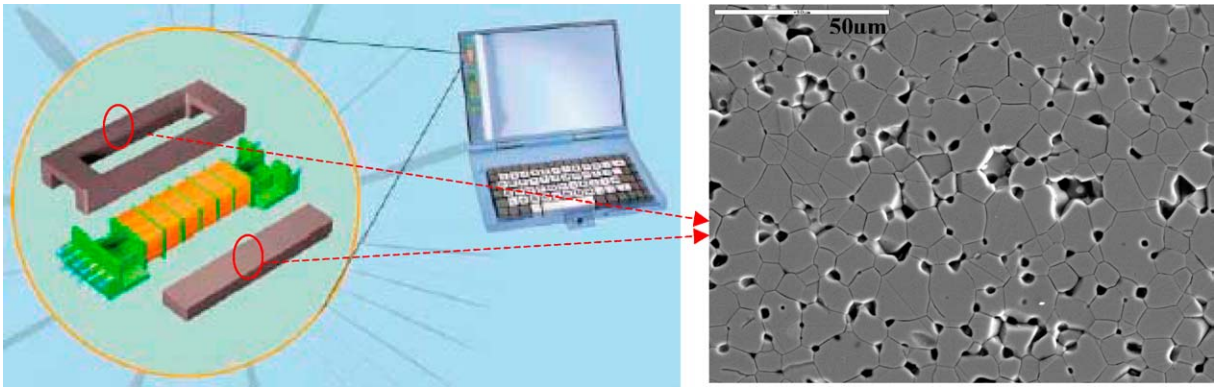

Fig. 1. Left: MnZn-ferrite ceramic components used for the construction of a "low-profile" power transformer to be placed in the screen section of a laptop. Right: Typical scanning electron microscope picture of a cross-section of a MnZn-ferrite indicating the basic characteristics of the polycrystalline structure (grains, grain-boundaries and pores).

losses are the sum of the power losses due to different and often simultaneously taking place loss mechanisms (e.g. hysteresis losses, eddy current losses, resonance losses etc.) [2]. For power applications that are usually characterized by relatively low frequencies (100 kHz) and high material magnetization (200 mT) almost 80–90% of the total power losses is due to hysteresis losses. Those are expressed by the well-known hysteresis loop area (i.e. the closed loop area of the magnetic field strength H versus magnetization B curve). For alternating currents that give rise to alternating magnetic fields the hysteresis losses are given by the relation:

$$w_h = \oint B dH \approx \frac{4\mu_0 v H_{\text{ampl}}^3}{3} \approx \frac{4v B_{\text{ampl}}^3}{3\mu_0^3 f(\mu_i)} \quad \text{Jm}^{-3}\text{per cycle} \qquad (1)$$

where H_{ampl} is the magnetic field strength amplitude, B_{ampl} is the material magnetization amplitude, v is a hysteresis loop constant, μ_0 is the magnetic permeability of vacuum (1.257×10^{-6} H m^{-1}), μ_i is the magnetic permeability of the material and $f(\mu_i)$ is a function proportionally dependent on the magnetic permeability.

The magnetic permeability of the ferrite material of the cubic spinel system is being approached by the relation:

$$\mu_i \approx \frac{2}{3}\frac{M_s}{H_\alpha} \qquad (2)$$

where M_s is the saturation magnetization of the material and H_α is the induced crystal anisotropy field which for cubic crystal symmetry is given by the relation:

$$H_\alpha = \frac{2K_1}{M_s} \qquad (3)$$

where K_1 is the magnetic anisotropy constant of the cubic crystal system.

The behavior of the power losses as a function of temperature, at constant frequency and magnetic field strength, is actually determined by the temperature behavior of the magnetic permeability μ_i (Eq. (1)), which in turn is determined by the temperature behavior of the crystal anisotropy K_1 (Eqs. (2) and (3)) that usually dominates over the temperature behavior of the saturation magnetization. Magnetostrictive effects in principle play also a role in determining the value of the magnetic permeability, however they are considered to be of minor quantitative influence when compared to that of the crystal anisotropy effects. The anisotropy constant K_1 physically represents the resistance or the energy barriers that the magnetic dipoles must overcome in order to leave their initial orientation and be aligned in agreement with the direction of the externally applied field. It depends on the crystal symmetry and on the interactions between the ions that occupy the various lattice sites. The smaller the anisotropy constant K_1, the easier the orientation of the magnetic dipoles to directions favorable to the direction of the external magnetic field, the higher the magnetic permeability and finally the lower the electromagnetic hysteresis losses. In MnZn-Ferrites the constant K_1 decreases with temperature until a certain temperature where it becomes zero ($T_{K_1=0}$). Subsequently and

at higher temperatures it takes negative values which physically means that the anisotropy field changes direction. The temperature $T_{K_1=0}$ coincides with the secondary maximum temperature of the magnetic permeability versus temperature curve and also with the temperature where the power losses exhibit a minimum. This may be also taken as an indication of the validity of the previous consideration that magnetostrictive effects, if present, are not of substantial quantitative influence. Current MnZn-ferrite materials for power applications are designed in such a way that the temperature of the power loss minimum falls between 80 and 100°C.

The electromagnetic power losses should be kept to an as possible low level because: (α) High losses may cause overheating of the component whose temperature may subsequently approach or exceed the materials Curie temperature. Above the Curie temperature the component becomes non-magnetic. (β) Low losses allow the design of smaller components at the same power efficiency, meeting therefore the miniaturization demands of the market.

Since the power losses of electromagnetic components are a strong function of temperature, usually they are optimized to a certain and generally accepted reference temperature which is the components steady state operation temperature of most applications. However, because of the continuously increasing number of electronic components per volume there is a dynamic shift of the previously mentioned optimum material design temperature simply because there is a dynamic shift in the steady state operation temperature of most devices. Nowadays power soft magnetic materials are optimized at 80–100°C where they show power losses of <300 mW/cm^3 when their windings are crossed by an alternating electric current of frequency 100 kHz which gives rise to the development of a magnetic field of 200 mT.

The previous outlined arguments bring about the necessity of the development of new materials designed for optimum performance at 140°C, where current materials exhibit losses of c.a. 600 mW/cm^3 at 100 kHz and 200 mT. Particularly in the automotive industry where the trend is observed for placing electronic control systems close to the engine where high temperatures are developed, the previous necessity is already a reality.

The development of such a material is described in this work.

Experimental

The shift of the minimum power loss temperature up to 140°C requires changes in the crystal structure of the material and shift of the $T_{K_1=0}$ temperature to 140°C [3]. Since the magnetic interactions between the ions of the lattice and the anisotropy field in the crystal structure of the type $(Mn_xZn_yFe^{2+}_{1-x-y})Fe^{3+}_2O_4$ depend significantly on the presence of Fe^{2+} ions in the structure, it has been considered worthwhile to study the effect of the Fe^{2+}concentration, on the magnetic properties. The variation is done: (α) either by varying the total amount of iron of the chemical composition (β) or by varying the partial pressure of oxygen during sintering.

Five synthesis experiments of MnZn-ferrites of the basic chemical compositions shown in Table 1 are made according to the experimental procedure shown in Fig. 2 [4, 5].

The amount and nature of dopants for the improvement of the microstructure and the electromagnetic properties are kept constant. Concerning the dopants and the mechanisms through which they influence the microstructure development it has been published elsewhere [6–8]. The presence of a certain amount of Fe^{2+} in the final material is considered necessary and it is determined by controlling the partial pressure of oxygen during sintering. The last is connected with the defect chemistry of the material with the relation:

$$2Fe^{3+} + \frac{3}{4}V_c + O^{2-} \leftrightarrow 2Fe^{2+} + \frac{1}{2}O_2 \qquad (4)$$

Equation (4) indicates that the partial pressure of oxygen in the sintering atmosphere is proportional to

Table 1. Chemical compositions of the laboratory synthesis experiments.

Exper. Nr.	Fe_2O_3 (%wt.)	MnO (% wt.)	ZnO (% wt.)	Corresponding formula of the type $AB_2O_4^*$
1	70.95	22.99	6.05	$(Mn_{0.755}Zn_{0.173}Fe^{2+}_{0.072})Fe^{3+}_2O_4$
2	70.85	23.09	6.05	$(Mn_{0.758}Zn_{0.173}Fe^{2+}_{0.069})Fe^{3+}_2O_4$
3	70.75	23.19	6.05	$(Mn_{0.761}Zn_{0.173}Fe^{2+}_{0.066})Fe^{3+}_2O_4$
4	70.65	23.29	6.05	$(Mn_{0.764}Zn_{0.173}Fe^{2+}_{0.063})Fe^{3+}_2O_4$
5	70.55	23.39	6.05	$(Mn_{0.767}Zn_{0.173}Fe^{2+}_{0.060})Fe^{3+}_2O_4$

*For the extraction of the chemical formula it has been assumed that all iron excess is placed at the tetrahedral A-sites of the cubic structure.

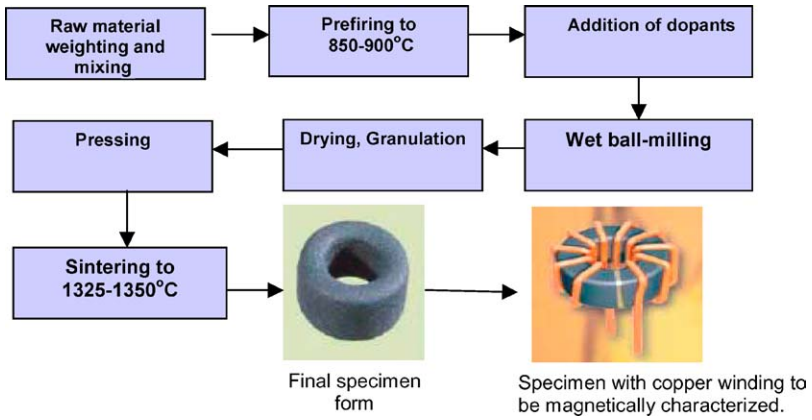

Fig. 2. Schematic diagram of the laboratory synthesis process of toroidally shaped MnZn-ferrite specimens.

the cation vacancy concentration (V_c) and inversely proportional to the concentration of divalent iron ions Fe^{2+} The main technological difficulty is that during the cooling stage of the sintering process the oxidation of the already formed divalent iron ions in the structure has to be avoided. This is done by controlling the partial pressure of oxygen during cooling, in specially constructed furnaces, so that in any temperature this corresponds to the partial pressure of oxygen dictated by the equilibrium constant of Eq. (4), $K_{\mathrm{p,equ}} = f(T)$.

In Fig. 3 the temperature and oxygen atmosphere profiles are shown of the two sintering programs used during the experiments and which correspond to two different top-temperatures and partial pressures of oxygen, resulting therefore to materials with identical

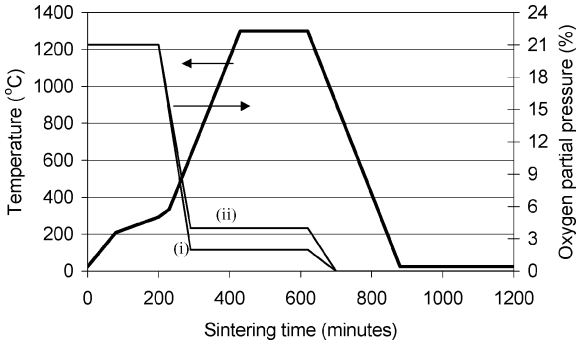

Fig. 3. Schematic diagram of the temperature and oxygen partial pressure profile during sintering. The same temperature curve corresponds to two atmospheric profiles indicated with (I) and (II), in the figure.

chemical composition but different oxygen and divalent iron content.

The electromagnetic properties have been measured with a Hewlett-Packard phase-impedance analyzer. The electromagnetic power losses have been measured from the alternating voltage along the copper winding of the ferrite specimens (Fig. 2) and from the real and imaginary part of the magnetic permeability.

Results and Discussion

The total electromagnetic power losses of the specimens with the chemical composition described in Table 1 (according to the sintering atmosphere profile i) as a function of temperature at a frequency of 100 kHz and magnetic field strength of 200 mT are shown in Fig. 4. Also in Fig. 4 are shown similar results at 100 kHz and 100 mT. As can be seen, the power loss minimum is being shifted to higher temperatures when moving from experiment 1 to experiment 5, reducing thus the Fe^{2+} amount of the composition and therefore shifting the zero passage of the magnetic anisotropy constant K_1. For example, experiment 1, which is a reference with the power loss minimum lying at 100°C, shows at 140°C, 100 kHz, 200 mT power losses of 500 mW/cc. The corresponding losses for experiment 5, with the minimum now lying at 140°C are 330 mW/cc. This means an improvement of 34%.

The electromagnetic losses corresponding to the atmospheric profile (ii) of the sintering process are shown in Fig. 5. In agreement to those mentioned previously, the increase of the partial pressure of oxygen during

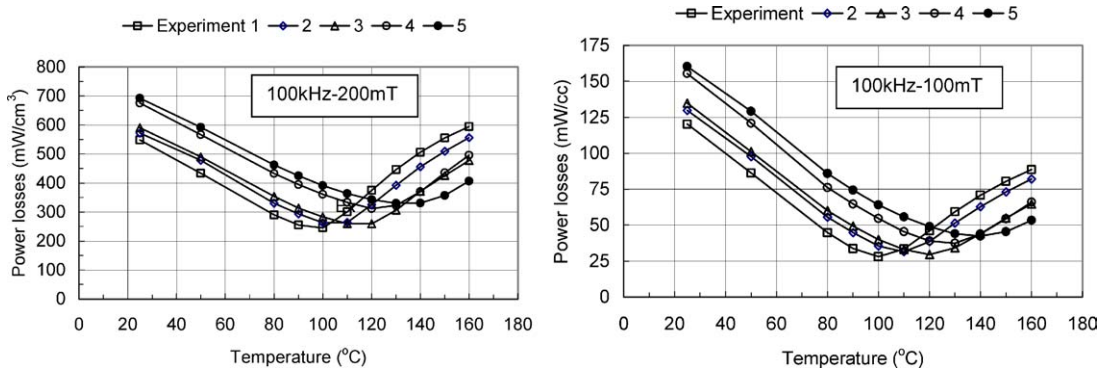

Fig. 4. Total electromagnetic power losses as a function of temperature for specimens of experiments 1–5 and according to the sintering atmosphere profile I.

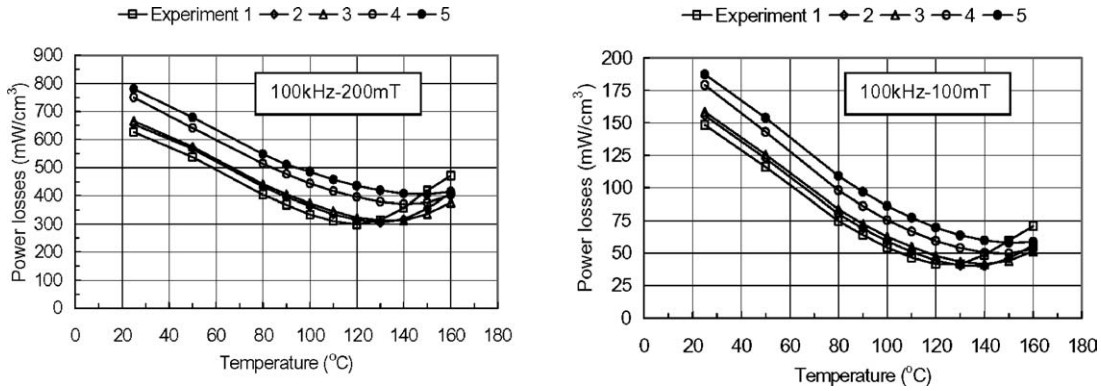

Fig. 5. Total electromagnetic power losses as a function of temperature for specimens of experiments 1–5 and according to the sintering atmosphere profile II.

sintering results, according to Eq. (4) to a decrease of the divalent iron percentage. Consequently the zero point of the anisotropy constant will be shifted to higher temperatures which means that also the total power loss minimum will be shifted to higher temperatures (e.g. this can be seen by comparing experiments of the same chemical composition but with different sintering atmospheres in Figs. 4 and 5). The saturation magnetization as a function of temperature for the two different atmospheric profiles during sintering are shown in Fig. 6.

From the previous results, two processing possibilities appear for the development of a magnetic core material with electromagnetic losses <350 mW/cm^3 (140°C, 100 kHz, 200 mT); either with a composition containing excess of iron sintered under reductive conditions (e.g. experiment 5, Fig. 4), or with a composition containing a higher iron excess which will be sintered in a less reductive atmosphere (e.g. experiments 2, 3, Fig. 5). According to the equilibrium described by Eq. (4), those two differently sintered materials will have also different cation vacancy concentrations into their structure. Consequently the cation diffusion coefficients (which are assumed to be proportional to the cation vacancy concentration) through their structure will be also different. In practice the (forced) diffusion and redistribution of cations (i.e. under the influence of a strong externally applied magnetic field) is related to the life time and the time stability of the component. Quantitatively this is given by the disaccommodation factor D_f of the specimen that expresses the variation of the initial magnetic

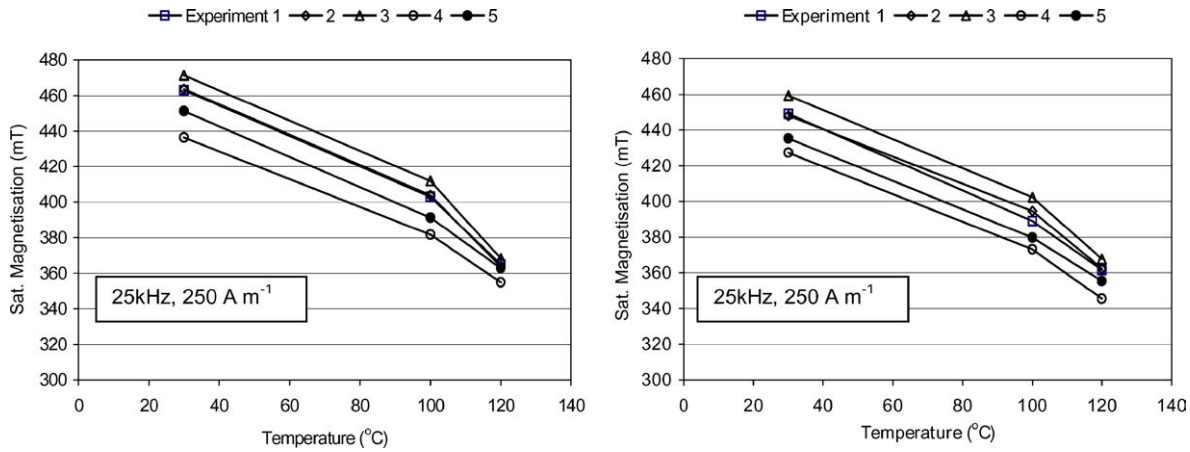

Fig. 6. Saturation magnetization as a function of temperature. Left: Samples are sintered according to sintering atmosphere profile (i). Right: Samples are sintered according to sintering atmosphere profile (ii).

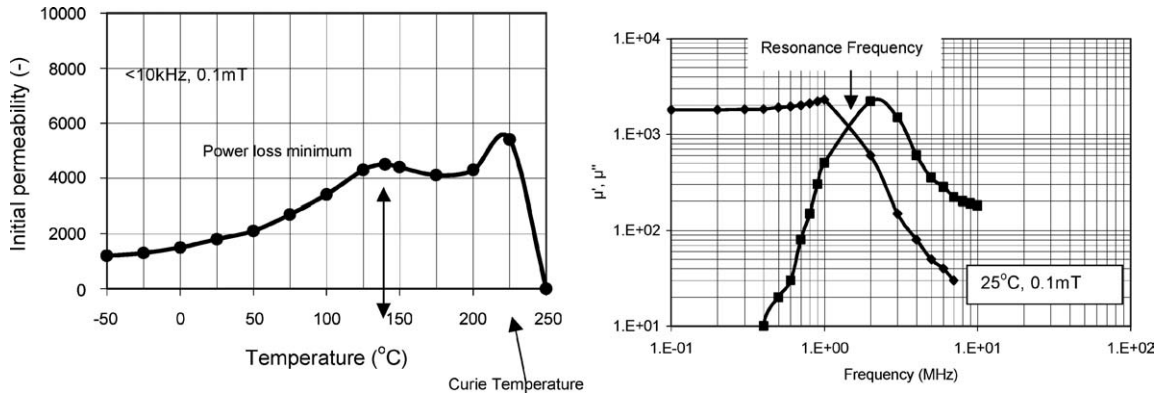

Fig. 7. Magnetic permeability characteristics of the specimens of experiment 5 (sintered according to atmosphere profile I). Left: The magnetic permeability as a function of temperature. The Curie temperature is determined to be 225°C. The power loss minimum temperature (140°C, Fig. 4) coincides with the temperature of the permeability secondary maximum in agreement with the consideration of the zero anisotropy constant temperature. Right: The real and imaginary parts of the complex magnetic permeability as a function of frequency. The resonance frequency is determined to be c.a. 1.5 MHz, while the real part of the permeability can be considered stable up to 500 kHz.

permeability from a moment t_1, where a strong magnetic disturbance is being given to the sample, to a moment t_2 (μ_1 and μ_2 are the corresponding values of the initial magnetic permeability) and is defined by the relation:

$$D_f = \frac{\mu_1 - \mu_2}{\mu_1^2 \log_{10}\left(\frac{t_2}{t_1}\right)}$$

Experimentally measured values of D_f for some selected experiments are shown in Table 2.

Based on the previous disaccommodation factor results and although experiments 2 and 3 showed the lowest electromagnetic power losses, experiment 5 was the one considered for further electromagnetic characterization. The results are shown in Figs. 7 and 8. Evaluation of all the results lead to the conclusion

Table 2. Values of the time stability parameter D_f (disaccommodation factor) and the corresponding power losses at 140°C, 100 kHz and 200 mT.

Experiment number	Sintering atmosphere profile	$D_f \times 10^6$	Losses (mW/cm^3), (140°C, 100 kHz, 200 mT)
5	(i)	16.7	330
2	(ii)	29.9	317
3	(ii)	31.3	312

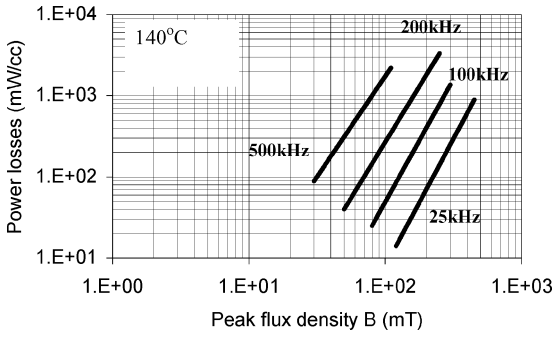

Fig. 8. The electromagnetic power losses of specimens of experiment 5 sintered according to atmosphere profile i, at 140°C and various frequency and peak induction conditions.

that this material fulfills all the requirements of the high temperature power applications. The subsequent agreement between laboratory and pilot batch experiments resulted to the introduction of this material into the regular production and its commercial availability.

Conclusions

- A new high-temperature magnetic material for power applications has been developed, optimized for steady state operation at 140°C, with electromagnetic power losses almost 34% lower than those of currently existing materials at the same temperature.
- Assuming the hysteresis losses as being the dominant loss mechanism the optimisation has been based on shifting the zero point temperature of the anisotropy constant to high temperatures. This has been done by reducing the Fe^{2+} ions into the lattice.
- Low oxygen partial pressures during sintering result to materials with low disaccommodation factors, probably due to the reduction of the cation vacancy concentration and the associated cation diffusion rates.
- The material described in this work has been successfully introduced into production and is currently available commercially.

References

1. A.J. Moulson and J.M. Herbert, *Electroceramics* (Chapman&Hall, London, 1995), Chap. 9.
2. E.C. Snelling, *Soft Ferrites, Properties and Applications* (Butterworth & Co, London, 1988) Chap., 2.
3. A. Goldman, *Handbook of Modern Ferromagnetic Materials* (Kluwer Academic Publishers, Boston, 1999), Chap. 3.
4. R. Mauczok and V. Zaspalis, *J. Eur. Cer. Soc.*, **20**, 2121 (2000).
5. V.T. Zaspalis, R. Mauczok, M. Kolenbrander, and J. Boerekamp, in *9th CimTec-World Ceramics Congress: Ceramics Getting into the 2000's*, edited by P. Vincenzini (Techna SrI., 1999), p. 401.
6. J.H. Han and D.Y. Kim, *J. Amer. Cer. Soc.*, **84**(3), 539 (2001).
7. A. Znidarsic and M. Drofenik, *J. Amer. Cer. Soc.*, **82**(2), 359 (1999).
8. V. Zaspalis, E. Antoniadis, E. Papazoglou, V. Tsakaloudi, and L. Nalbandian, *J. Magn. Magn. Mater.*, **98**, 250, (2002).